Plasma GFAP is an early marker of amyloid-β but not tau pathology in Alzheimer's disease

Joana B. Pereira,[1,2] Shorena Janelidze,[2] Ruben Smith,[2,3] Niklas Mattsson-Carlgren,[2,3,4] Sebastian Palmqvist,[1,3] Charlotte E. Teunissen,[5] Henrik Zetterberg,[6,7,8,9] Erik Stomrud,[2,10] Nicholas J. Ashton,[6,11,12,13] Kaj Blennow[6,7] and Oskar Hansson[2,10]

Abstract

Although recent clinical trials targeting amyloid-β (Aβ) in Alzheimer's disease (AD) have shown promising results, there is increasing evidence suggesting that understanding alternative disease pathways that interact with Aβ metabolism and amyloid pathology might be important to halt the clinical deterioration. In particular, there is evidence supporting a critical role of astroglial activation and astrocytosis in AD. However, to this date, no studies have assessed whether astrocytosis is independently related to either Aβ or tau pathology, respectively, *in vivo*. To address this question, we determined the levels of the astrocytic marker glial fibrillary acidic protein (GFAP) in plasma and cerebrospinal fluid (CSF) of 217 Aβ-negative cognitively unimpaired individuals, 71 Aβ-positive cognitively unimpaired individuals, 78 Aβ-positive cognitively impaired individuals, 63 Aβ-negative cognitively impaired individuals and 75 patients with a non-AD neurodegenerative disorder from the Swedish BioFINDER-2 study. Subjects underwent longitudinal Aβ (^{18}F-flutemetamol) and tau (^{18}F-RO948) positron emission tomography (PET) as well as cognitive testing. We found that plasma GFAP concentration was significantly increased in all Aβ-positive groups compared with subjects without Aβ pathology ($p<0.01$). In addition, there were significant associations between plasma GFAP with higher Aβ-PET signal in all Aβ-positive groups, but also in cognitively normal individuals with normal Aβ values ($p<0.001$), which remained significant after controlling for tau-PET signal. Furthermore, plasma GFAP could predict Aβ-PET positivity with an area under the curve of 0.76, which was greater than the performance achieved by CSF GFAP (0.69) and other glial markers (CSF YKL-40: 0.64, sTREM2: 0.71). Although correlations were also observed between tau-PET and plasma GFAP, these were no longer significant after controlling for Aβ-PET. In contrast to plasma GFAP, CSF GFAP concentration was significantly increased in non-AD patients compared to other groups ($p<0.05$) and correlated with Aβ-PET only in Aβ-positive cognitively impaired individuals

(p=0.005). Finally, plasma GFAP was associated with both longitudinal Aβ-PET and cognitive decline, and mediated the effect of Aβ-PET on tau-PET burden, suggesting that astrocytosis secondary to Aβ aggregation might promote tau accumulation. Altogether, these findings indicate that plasma GFAP is an early marker associated with brain Aβ pathology but not tau aggregation, even in cognitively normal individuals with a normal Aβ status. This suggests that plasma GFAP should be incorporated in current hypothetical models of AD pathogenesis and be used as a non-invasive and accessible tool to detect early astrocytosis secondary to Aβ pathology.

Author affiliations:

1 Division of Clinical Geriatrics, Department of Neurobiology, Care Sciences and Society, Karolinska Institute, Stockholm, Sweden

2 Clinical Memory Research Unit, Department of Clinical Sciences Malmö, Lund University, Sweden

3 Department of Neurology, Skåne University Hospital, Lund University, Lund, Sweden

4 Wallenberg Center for Molecular Medicine, Lund University, Lund, Sweden

5 Neurochemistry Laboratory, Department of Clinical Chemistry, Amsterdam Neuroscience, Amsterdam University Medical Centers, Amsterdam, The Netherlands

6 Institute of Neuroscience and Physiology, Department of Psychiatry and Neurochemistry, the Sahlgrenska Academy at the University of Gothenburg, Mölndal, Sweden

7 Clinical Neurochemistry Laboratory, Sahlgrenska University Hospital, Mölndal, Sweden

8 Department of Neurodegenerative Disease, UCL Institute of Neurology, London, UK

9 UK Dementia Research Institute at UCL, London, UK

10 Memory Clinic, Skåne University Hospital, Malmö, Sweden

11 Wallenberg Centre for Molecular and Translational Medicine, The Sahlgrenska Academy at the University of Gothenburg, Gothenburg, Sweden

12 Institute of Psychiatry, Psychology and Neuroscience, King's College London, Maurice Wohl Clinical Neuroscience Institute, London, UK

13 NIHR Biomedical Research Centre for Mental Health and Biomedical Research Unit for Dementia at South London & Maudsley NHS Foundation, London, UK

Correspondence to: Joana B. Pereira

Division of Clinical Geriatrics, Department of Neurobiology, Care Sciences and Society, Karolinska Institute, 141 83 Huddinge, Sweden

E-mail: joana.pereira@ki.se

Correspondence may also be addressed to: Oskar Hansson

Clinical Memory Research Unit, Department of Clinical Sciences, Lund University, SE-20502 Malmö, Sweden

E-mail: Oskar.Hansson@med.lu.se

Running title: GFAP is an early marker of Aβ

Keywords: astrocytosis; GFAP; Aβ-PET; tau-PET; cognition

Abbreviations: Aβ = amyloid-β**;** GFAP = astrocytic marker glial fibrillary acidic protein**;** PET = positron emission tomography**;** CSF = cerebrospinal fluid**;** MMSE = mini-mental state examination**;** sTREM2 = soluble triggering receptor expressed on myeloid cells 2**;** SUVR = standardized uptake value ratio

Introduction

There is increasing evidence suggesting that the pathogenesis of Alzheimer's disease (AD) is not restricted to amyloid-β (Aβ) plaques and tau tangles but also includes strong interactions with immunological mechanisms.[1] In line with this, astrocyte reactivity or astrocytosis is a well-known pathological process that is commonly found surrounding Aβ plaques in the brains of AD patients.[2] Although the exact role of astrocytosis is not clear, several studies have shown that reactive astrocytes penetrate Aβ plaques with their processes, possibly in an attempt to isolate the plaques from the surrounding neuropil and phagocytize them.[3,4] This close relationship between astrocytes and plaques has been further supported by neuropathological reports showing that reactive astrocytes follow the same spatial distribution of Aβ plaques in the association cortex of AD patients.[5,6]

In contrast to the association between astrocytosis and Aβ plaques, the relationship between reactive astrocytes and tau tangles has been less investigated. The few available studies that have assessed this showed that reactive astrocytes also interact with tau, but only in advanced stages of AD by penetrating the extracellular ghost tau tangles.[7,8] In addition, it has also been found that the association between reactive astrocytes and tau tangles parallels the progression of AD,[9] however it is not clear whether this association is independent of Aβ plaques, which are normally present in the brains of patients with AD who have tau tangles.

Thanks to the development of biomarkers to measure astrocytosis, such as the glial fibrillary acidic protein (GFAP), it is now possible to address this question and disentangle the underlying effects of reactive astrocytes on both Aβ and tau pathology *in vivo*. In particular, the recent assays that allow measuring the concentrations of GFAP in the blood have already demonstrated the potential of plasma GFAP in distinguishing different stages of AD and detecting Aβ positivity on positron emission tomography (PET).[10-18] However, no study has yet assessed whether plasma GFAP is also associated with tau-PET burden. Moreover, to this date, it is not known whether astrocytosis is independently related to both Aβ and tau pathology, respectively, *in vivo*. This is important for several reasons including the fact that Aβ and tau pathology are not independent processes, showing a synergistic and complex interaction over the course of AD that may become exacerbated in the presence of other pathological processes such as astrocytosis.[19] Thus, a better understanding of when reactive astrocytes emerge in the progression of AD and how they relate to the classic AD pathologies

is crucial to determine their clinical value as diagnostic or prognostic tools as well as to inform the development of anti-inflammatory drugs in clinical trials.

Moreover, to our knowledge, no studies have yet compared the performance of plasma and CSF GFAP in detecting AD pathology to other glial markers such as the soluble triggering receptor expressed on myeloid cells 2 (sTREM2) or chitinase 3-like 1 (YKL-40). TREM2 is an innate immune receptor expressed by microglia, which is associated with cytokine release, phagocytosis, proliferation and migration.[20] The AD-associated TREM2 variants seem to cause loss of function of TREM2 and reduce the ability of microglia to respond to toxic metabolites and clear them from the brain.[21] Although initial studies examining the differences in CSF sTREM2 concentrations between patients with AD and healthy individuals did not show any differences,[22] or showed reduced concentrations in patients with AD compared with healthy controls,[23] later studies have found higher concentrations of CSF sTREM2 in patients with mild cognitive impairment and Alzheimer's disease.[24-29] On the other hand, YKL-40 is a secreted glycoprotein that is involved in the activation of the innate immune system as well as cell processes in relation to extracellular matrix remodeling.[30-33] During neuroinflammatory processes, YKL-40 increases its expression in reactive astrocytes and microgial cells.[34] Several studies have found that YKL-40 is increased in the CSF of patients with mild cognitive impairment and AD dementia as well as cognitively normal individuals with amyloid pathology.[35-37] Moreover, YKL-40 levels have been found to be elevated in mutations carriers of autosomal dominant AD 15 to 19 years before estimated symptom onset, shortly after the beginning of brain amyloid accumulation.[38]

The aim of this study was to assess whether plasma and cerebrospinal fluid (CSF) GFAP concentrations change across different stages of AD and investigate the independent relationships between these markers with Aβ and tau pathology measured using ^{18}F-flutemetamol PET and ^{18}F-RO948 PET, respectively. Moreover, we compared the performance of GFAP to CSF sTREM2 and CSF YKL-40 to detect Aβ and tau-PET pathology in order to determine the specificity of our findings. We also evaluated the prognostic ability of baseline GFAP markers to predict longitudinal changes in PET burden and cognitive decline. Finally, we conducted sensitivity analyses in a separate group of patients with non-AD disorders to assess the ability of GFAP markers to detect Aβ-positivity determined with CSF Aβ42/40.

Materials and methods

Participants

This study included 504 individuals from the Swedish BioFINDER-2 cohort (NCT03174938), a prospective study with the aim of developing new biomarkers for the early diagnosis of AD and other neurodegenerative disorders. All participants were recruited at Skåne University Hospital and the Hospital of Ängelholm in Sweden between 2017 and 2020 and included cognitively unimpaired controls, patients with mild cognitive impairment, AD dementia and non-AD disorders.[40] Further details regarding the inclusion and exclusion criteria of the subjects included in the different BioFINDER-2 cohorts can be found in the Supplementary Material.

For the purposes of this study, only subjects with baseline plasma and CSF levels of GFAP in addition to other glial markers (YKL-40, sTREM2), ^{18}F-flutemetamol PET, ^{18}F-RO948 PET and mini-mental examination scores (MMSE) were included. In addition, a subsample (n = 196) also underwent longitudinal PET imaging and cognitive assessments (n = 185). Finally, a group of 75 patients with non-AD neurodegenerative disorders without ^{18}F-flutemetamol PET data was also included. This group included 21 patients with dementia with Lewy bodies, 14 patients with unspecified dementia, 12 with vascular dementia, 10 with frontotemporal dementia, 6 with progressive supranuclear palsy, 5 with Parkinson's disease dementia, 4 with semantic dementia, 1 with progressive non-fluent aphasia, 1 with Parkinson's disease without dementia and 1 with amyotrophic lateral sclerosis.

Plasma and cerebrospinal fluid biomarkers

Plasma and CSF samples were collected in the morning during the same visit, with participants nonfasting.[40] Blood was collected in six EDTA-plasma tubes and centrifuged (2,000 g, + 4 ° (C) for 10 min. Following centrifugation, plasma was aliquoted into 1.5-ml polypropylene tubes (1 ml plasma in each tube) and stored at −80 °C within 30–60 min of collection. CSF was collected by lumbar puncture and stored at -80◦C in polypropylene tubes.[40] The following assays were used to measure the different biomarkers of interest to this study: GFAP Simoa Discovery kits for HD-X (Quanterix®, Billerica, MA, USA) for plasma GFAP; Elecsys assays (NeuroToolKit robust prototype, Roche Diagnostics) for CSF GFAP, YKL-40 and sTREM2; and Meso Scale Discovery immunoassays (MSD; Rockville, MD,

USA) for CSF Aβ42 and CSF Aβ40.[40,41] Considering that GFAP in plasma and CSF were measured using different platforms we compared these assays to each other in a separate cohort, finding a high agreement in plasma (Supplementary information). In all subjects, Aβ status was established using CSF Aβ42/40 levels with a previously established cutoff of 0.0752 defined with mixture modeling[42], because CSF Aβ42/40 was available in all cases (by study design), whereas Aβ-PET was only available in non-demented cases.[40] We would like to highlight that the criteria for Aβ-PET availability was specific for the BioFINDER-2 cohort, which is the cohort we used in the current study (in BioFINDER-1, Aβ-PET scans were also available for AD demented cases).

Imaging acquisition and preprocessing

All subjects underwent ^{18}F-flutemetamol PET and ^{18}F-RO948 PET on General Electrics Discovery MI scanners. ^{18}F-flutemetamol PET images were acquired 90 to 110 minutes after injection of 185 MBq 18F-flutemetamol and ^{18}F-RO948 PET images were acquired 70 to 90 minutes after injection of 370 MBq ^{18}F-RO948. Images were reconstructed using VPFX-S (ordered subset expectation maximization combined with corrections for time-of-flight and point spread function).

All ^{18}F-flutemetamol and ^{18}F-RO948 PET images were motion-corrected, time-averaged and coregistered to their corresponding skull stripped, longitudinally preprocessed T1-weighted images. ^{18}F-Flutemetamol scans were normalized using a reference region that included the whole cerebellum, brain stem and eroded subcortical white matter,[43] whereas ^{18}F-RO948 images were normalized by a reference region consisting of the inferior cerebellar gray matter.[44]

For ^{18}F-flutemetamol images, we calculated the standardized uptake value ratios (SUVR) for a global composite region that included the caudal anterior cingulate, frontal, lateral parietal and lateral temporal gyri.[43] In contrast, for ^{18}F-RO948 PET images we calculated the SUVRs for three composite regions that corresponded to Braak stages I-II (entorhinal cortex), III-IV (parahippocampal, fusiform, amygdala, inferior temporal, middle temporal) and V-VI (posterior cingulate, caudal anterior cingulate, rostral anterior cingulate, precuneus, inferior parietal, superior parietal, insula, supramarginal, lingual, superior temporal, medial orbitofrontal, rostral middle frontal, lateral orbitofrontal, caudal middle frontal, superior frontal, lateral occipital, precentral gyrus, postcentral gyrus and paracentral gyrus).[45] Finally,

voxel-wise analyses were conducted using the preprocessed ^{18}F-flutemetamol and ^{18}F-RO948 PET images using the statistical parametric mapping software SPM12 (https://www.fil.ion.ucl.ac.uk/spm/) after applying a smoothing kernel of 8 mm.

Statistical analyses

Logarithmic or reciprocal transformations were applied to the variables that were not normally distributed. Then, a set of pairwise t-tests was used to compare plasma and CSF GFAP levels between Aβ-negative cognitively unimpaired (CU), Aβ-positive CU, Aβ-positive cognitively impaired (CI), Aβ-negative CI and non-AD patients, while adjusting for age and sex, and using CSF Aβ42/Aβ40 to determine the Aβ status.

To assess the ability of CSF and plasma GFAP markers to predict Aβ and tau pathology, we used two different approaches: one based on regions of interest (ROI) and the other one based on whole brain voxel-wise analyses. For the first approach, we built separate linear regression models with plasma or CSF GFAP as the dependent variable and global Aβ, tau stages I-II, tau stages III-IV or tau stages V-VI SUVRs as the outcome, controlling for age and sex. In all models, we verified that the residuals were normally distributed, there was no heteroscedasticity and no multicollinearity. For the second approach, we conducted voxel-wise regression analyses using plasma or CSF GFAP as the dependent variable and the smoothed preprocessed ^{18}F-Flutemetamol or ^{18}F-RO948 PET images as the outcome, including age and sex as covariates. All ROI-based and voxel-wise analyses were carried out in Aβ-negative CU, Aβ-positive CU, all CU subjects, Aβ-positive CI and Aβ-negative CI individuals.

For the PET variables showing a significant relationship with plasma and CSF GFAP, we performed three additional analyses. First, we built spline models[46] to determine the trajectories of GFAP markers as a function of higher PET burden over the course of AD. Due to previous evidence showing that AD progresses from Aβ-negative CU to Aβ-positive CU and finally Aβ-positive CI,[47] we only included these groups in this analysis. Secondly, to determine the impact of astrocytosis on the relationship between the two classical AD hallmarks, we conducted mediation analyses to test whether the relationship between Aβ-PET and tau-PET burden could be explained by a mediation of GFAP, while controlling for age and sex. The significance of the mediation was assessed by calculating bias-corrected 95% confidence intervals (CIs) using bootstrapping (500 resamples). Thirdly, to establish the

area under the curve, sensitivity, specific and accuracy of GFAP markers in determining an Aβ-positive status, we calculated receiver-operating curves using a bootstrap procedure with 1000 permutations in the groups who had ^{18}F-flutemetamol PET data: all CU subjects, all CI subjects and in the whole sample. Since non-AD patients did not have ^{18}F-flutemetamol scans, the analyses in this group were conducted using CSF Aβ42/40 to determine Aβ-positivity. All receiver-operating curve analyses included YKL-40 and sTREM2 to assess the value of GFAP with respect to other glial markers and their performance was compared using the DeLong test.

Finally, to test whether plasma and CSF GFAP markers were associated with longitudinal changes in cognition and PET burden we applied linear mixed effect models. These models used longitudinal MMSE scores or PET SUVRs as a dependent variable and the GFAP markers, time, age, sex as fixed effects. We also included the interaction between biomarker levels and time (together with the main effects), and random effects for intercepts. Separate models were built for plasma and CSF GFAP, which were ran in all CU subjects, all CI individuals and in the whole sample. The models ran across the entire sample included Aβ and cognitive status as additional covariates. In addition, to assess whether the effects of GFAP on cognition were independent of Aβ-PET, longitudinal changes in Aβ-PET burden were also included as a covariate in a secondary analysis.

Statistical analyses were carried out using SPSS 25.0 (IBM Corp., Armonk, NY, USA), R (version 3.5.1) or SPM12. The analyses conducted in R and SPSS were adjusted for multiple comparisons using false discovery rate (FDR) corrections ($q < 0.05$, two-tailed).[48] Similarly, the voxel-wise analyses using PET images were adjusted for multiple comparisons with topological FDR corrections in SPM12 ($p < 0.05$, two-tailed).[49]

Data availability

Anonymized data will be shared by request from a qualified academic investigator for the sole purpose of replicating procedures and results presented in the article and as long as data transfer is in agreement with EU legislation on the general data protection regulation and decisions by the Ethical Review Board of Sweden and Region Skåne, which should be regulated in a material transfer agreement.

Results

Study participants

In total, 504 participants were included in this study, of which 217 were Aβ-negative CU, 71 were Aβ-positive CU, 78 were Aβ-positive CI (mild cognitive impairment or AD dementia), 63 were Aβ-negative CI (mild cognitive impairment) and 75 had a non-AD neurodegenerative disorder (Table 1). There was a moderate correlation between plasma GFAP and CSF GFAP in the entire sample ($r = 0.582$, $p < 0.001$). Both plasma and CSF GFAP were positively associated with age (plasma GFAP: $r = 0.528$, $p < 0.001$; CSF GFAP: $r = 0.602$, $p < 0.001$) and women had higher plasma GFAP values compared to men ($F_{(2,502)} = 6.24$, $p = 0.013$) in the whole sample.

Plasma GFAP concentration is increased across different AD stages, whereas CSF GFAP concentration is increased in non-AD disorders

Our findings revealed that plasma GFAP concentration was lowest in Aβ-negative CI, followed by Aβ-negative CU, Aβ-positive CU and Aβ-positive CI individuals (Figure 1A). The group comparisons showed that both Aβ-positive CU and CI individuals showed elevated plasma GFAP levels compared to the Aβ-negative CU group ($F_{(2,286)} = 8.33$, $p = 0.004$, $F_{(2,293)} = 12.90$, $p < 0.001$, respectively) and to the Aβ-negative CI group ($F_{(2,132)} = 18.06$, $p < 0.001$; $F_{(2,139)} = 24.14$, $p < 0.001$, respectively). These findings suggest that plasma GFAP is elevated in individuals with Aβ pathology.

In contrast to plasma GFAP, CSF GFAP was significantly elevated in patients with a non-AD disorder compared to both Aβ-negative CU individuals ($F_{(2,290)} = 9.61$, $p = 0.002$) and Aβ-positive CU individuals ($F_{(2,144)} = 5.71$, $p = 0.018$) (Figure 1B). These findings suggest that CSF GFAP might be sensitive to different underlying pathological processes unrelated to AD and might be better suited for the detection of non-AD disorders.

Plasma and CSF GFAP concentrations are associated with Aβ-PET independently of tau-PET burden

To assess whether GFAP biomarkers were associated with the severity of Aβ deposition, we built linear regression models using global Aβ-PET SUVR values as the outcome in addition to plasma or CSF GFAP as the predictors. We found that increasing GFAP levels in plasma were associated with greater global Aβ-PET burden in all CU individuals ($t = 4.24$, $p < 0.001$) (Figure 2A), Aβ-negative CU individuals ($t = 2.31$, $p = 0.022$) (Figure 2B), Aβ-positive CU individuals ($t = 2.11$, $p = 0.039$) (Figure 2C) and Aβ-positive CI individuals ($t = 2.88$, $p = 0.005$) (Figure 2D). These results were further confirmed by the voxel-wise analyses, which showed that plasma GFAP correlated with higher Aβ-PET deposition in several neocortical regions in all CU individuals (Figure 3A) as well as in Aβ-positive CU individuals (Figure 3B). In contrast to plasma GFAP, CSF GFAP only showed a significant association with higher Aβ-PET deposition in Aβ-positive CI subjects ($t = 2.92$, $p = 0.005$) (Figure 2E). To determine whether these results were independent of tau pathology, we repeated all of the above analyses including tau-PET SUVR values of different Braak stage ROIs as covariates. These analyses showed that Aβ-PET burden was still related to increased plasma GFAP in the same groups (all CU individuals: $t = 4.50$, $p < 0.001$; Aβ-negative CU individuals: $t = 2.70$, $p = 0.007$; Aβ-positive CU individuals: $t = 2.32$, $p = 0.024$; Aβ-positive CI individuals: $t = 2.08$, $p = 0.041$) and to increased CSF GFAP in Aβ-positive CI individuals ($t = 2.18$, $p = 0.032$), after controlling for tau-PET.

To assess whether the GFAP biomarkers were associated with the severity of tau deposition, we built linear regression models using the tau-PET SUVR values across different Braak stage ROIs as the outcome in addition to plasma or CSF GFAP as the predictors. We found that increasing plasma GFAP levels were only associated with tau-PET burden across Braak stages III-IV and V-VI in Aβ-positive CI individuals (III-IV: $t = 2.86$, $p = 0.006$; V-VI: $t = 2.97$, $p = 0.004$). However, these associations lost their significance after including global Aβ-PET as a covariate (III-IV: $t = 1.60$, $p = 0.114$; V-VI: $t = 2.00$, $p = 0.050$), indicating that they were not independent of Aβ pathology.

Plasma GFAP concentration shows early increases with Aβ-PET burden

To determine the trajectories of plasma and CSF GFAP concentrations over the course of AD, we fitted spline models for these markers using global Aβ-PET SUVR as a proxy for time. These analyses did not include non-AD patients or Aβ-negative CI individuals since they are not considered to be part of the AD spectrum.[47] The results of these analyses revealed that both models were significant, with the one having plasma GFAP as a predictor showing a better model fit (r2: 0.21, $p < 0.001$) compared to the one with CSF GFAP (r2: 0.14, $p < 0.001$). These differences between models were statistically significant ($F = 15.92$, $p < 0.001$). The trajectories of these models revealed initial increases for both plasma GFAP (Figure 4A) and CSF GFAP (Figure 4B), which continued rising after reaching the threshold for Aβ-PET positivity and then later came to a plateau. Despite showing similar trajectories, when we compared the splines of plasma and CSF GFAP, we could observe that plasma GFAP showed steeper initial increases, overcoming CSF GFAP levels even before Aβ-PET positivity (Figure 4C). These results indicate that plasma GFAP might exhibit greater changes with increasing Aβ pathology during AD compared to CSF GFAP.

Plasma GFAP may partially mediate the relationship between Aβ-PET and tau-PET over the course of AD

To further investigate the role of astrocytosis in relation to the classical AD pathologies over the course of the disease we conducted mediation analyses in all CU subjects as well as Aβ-positive CI individuals. These analyses showed that plasma GFAP mediated the effect between global Aβ-PET and both tau-PET stages I-II (-0.027, 95% CI: 0.00 to -0.056, P = 0.035) and stages III-IV (-0.027, 95% CI: -0.056 to -0.01, P = 0.010) in CU individuals. Moreover, plasma GFAP also mediated the effects between global Aβ-PET and tau-PET stages V-VI (0.131, 95% CI: 0.00 to 0.33, P = 0.046) in CI individuals. These findings suggest that astrocytosis secondary to Aβ accumulation might be one the factors contributing to tau accumulation in AD.

Plasma GFAP identifies an Aβ-positive status more accurately than CSF GFAP and other glial markers

To determine the performance of the glial biomarkers (GFAP, YKL-40 and sTREM2) to detect Aβ positivity, we conducted receiver-operating curve analyses in the whole sample, all CU individuals, all CI individuals as well as non-AD patients, regardless of their Aβ status, which were defined using Aβ-PET or CSF Aβ42/40 (non-AD patients only) (Table 2). These analyses showed that plasma GFAP showed an area under the curve of 0.761 in the whole sample (Figure 5A), 0.754 in all CU individuals (Figure 5B), 0.779 in all CI individuals (Figure 5C) and 0.755 in non-AD patients (Figure 5D). These performances were significantly better than the ones achieved by CSF GFAP ($Z = 2.68$, $p = 0.007$), CSF sTREM2 ($Z = 3.31$, $p < 0.001$) and almost CSF YKL-40 ($Z = 1.77$, $p = 0.077$) in the whole sample; by CSF GFAP ($Z = 2.24$, $p = 0.024$) in CU individuals; by CSF GFAP ($Z = 2.24$, $p = 0.025$), CSF sTREM2 ($Z = 3.08$, $p = 0.002$) and CSF YKL-40 ($Z = 2.72$, $p = 0.006$) in CI individuals; and by CSF YKL-40 ($Z = 2.42$, $p = 0.016$) and almost CSF sTREM2 ($Z = 1.80$, $p = 0.072$) in non-AD patients. Altogether, these analyses indicate that plasma GFAP can detect an Aβ positive status more accurately than the other glial markers.

Plasma GFAP concentration is associated with longitudinal Aβ accumulation determined by PET

For the subsample that underwent longitudinal Aβ-PET (n = 196, number of visits: **M = 2**, follow-up time: M = 1.7 years, IQR = 0.3), we used linear mixed models to evaluate whether the GFAP markers were also associated with Aβ changes over time in a neocortical composite region. These analyses showed that plasma GFAP predicted longitudinal Aβ deposition in the whole sample ($t = 2.888$, $p = 0.004$) (Figure 6A), whereas CSF GFAP did not ($t = 1.478$, $p = 0.141$), after controlling for age, sex, baseline Aβ status and presence of cognitive impairment. Notably, these analyses remained significant after adjusting also for tau-PET burden ($t = 2.905$, $p = 0.004$), indicating they were independent of tau pathology. However, no significant results when the analyses were conducted in the CU and CI groups separately.

Plasma and CSF GFAP concentrations are associated with longitudinal cognitive decline

For the subsample that underwent longitudinal cognitive assessment (total n = 185, CU = 133, CI = 52, number of visits: M = 3, follow-up time: M = 1.9 years, IQR = 0.7), we also used linear mixed models to evaluate whether the GFAP markers were associated with cognitive changes over time. These analyses showed that both plasma GFAP and CSF GFAP predicted cognitive decline in the whole cohort, even after adjusting for longitudinal Aβ-PET changes (plasma GFAP: t = -3.303, p = 0.001; CSF GFAP: t = -2.485, p = 0.014) (Figure 6B, 6C). These results suggest that, in addition to being a marker of Aβ pathology, astrocytosis could have an independent negative impact on longitudinal cognition. No significant results were found when the analyses were conducted in the CU and CI groups separately.

Discussion

Although emerging evidence suggests that inflammation has a causal role in AD,[11-18] the detection of inflammatory markers has not yet been established as a valuable method for the early diagnosis and monitoring of AD patients.[1] Our findings show that plasma GFAP holds great potential as an early and specific marker of Aβ deposition even during the earliest stages of AD. Moreover, we found that plasma GFAP was a prognostic marker of both longitudinal Aβ accumulation and cognitive decline and a mediator of the effects of Aβ-PET on tau-PET burden. In light of the invasiveness of lumbar punctures for CSF and the high cost of PET imaging, our findings suggest that plasma GFAP could become a widely available screening tool to identify astrocytosis in early AD. Moreover, it could also be used to evaluate the effects of anti-Aβ therapies on glial activation as well as to better understand the role of astrocytosis over the course of AD.

Activated glia in the form of reactive astrocytes is one of the most prominent neuropathological features of AD, being normally found surrounding Aβ plaques in postmortem brain tissue.[50] The role of these reactive astrocytes has been debated over the past few years, with some studies suggesting they are part of an endogenous defensive mechanism to eliminate the plaques, whereas others defend that their persistent activation induces a toxic inflammatory process that contributes to worsening AD progression.[51] Regardless of their role, several studies have used biomarkers such as GFAP to measure astrocytosis *in vivo* in the CSF or more recently in the blood plasma. Although studies

assessing GFAP in CSF have reported somewhat inconsistent findings across different stages of AD,[52,53] recent studies on plasma GFAP showed more promising results. In particular, elevated plasma GFAP was recently found in subjects with subjective cognitive decline, mild cognitive impairment and AD dementia with a positive Aβ-PET scan.[15] In addition, an association between longitudinal plasma GFAP and conversion to dementia was also found in a prospective clinical cohort, highlighting its potential value as a prognostic tool.[54] In the current study, we extend these previous findings by showing that plasma GFAP is not only elevated in subjects with Aβ pathology but also correlates with continuous Aβ-PET values, even in individuals with normal CSF Aβ42/40 levels. Interestingly, when we conducted our analyses at the voxel-level we found that elevated plasma GFAP was associated with higher Aβ-PET burden in neocortical regions where Aβ accumulation is normally observed in AD both in all CU as well as Aβ-positive CU individuals. This result is in agreement with previous studies showing that astrocytes show dynamic changes over the course of AD, with reactive astrocytes being more prominent in earlier disease stages.[51] In addition, this result is also in line with a previous report showing that reactive astrocytes follow the same spatial distribution of Aβ plaques in the association cortex of AD patients.[5]

Compared to Aβ plaques, the potential associations between reactive astrocytes and neurofibrillary tangles have been much less studied. Immunohistochemical and electron microscopy studies have shown that reactive astrocytes can also penetrate with their processes the extracellular ghost tangles in the midst of the neuropil in advanced AD.[7,8] Moreover, in another study, a significant linear rise of astrocytosis in the vicinity of neurofibrillary tangles was found with increasing AD progression, although this relationship was weaker than the one observed between astrocytosis and Aβ plaques.[55] Finally, in a study using autoradiography, tau deposits were observed in similar brain areas as activated astrocytes, supporting a pathological interconnection.[56] To our knowledge, no studies have assessed whether astrocytic markers such as plasma and CSF GFAP are associated with *in vivo regional* tau-PET pathology in the course of AD. Here, we show that greater tau-PET signal in middle and late Braak stages was associated with increasing plasma GFAP in Aβ-positive CI individuals. However, when these associations were adjusted for Aβ-PET burden their significance was lost, in contrast to the correlations between plasma GFAP and Aβ-PET, which remained unchanged after adjusting for tau-PET signal. These findings indicate that astrocytosis measured by initial increases in GFAP is specifically associated with Aβ

pathology, challenging previous assumptions that both Aβ and tau pathology can trigger reactive astrocytes in AD.[6,55]

In contrast to plasma GFAP, CSF GFAP was only associated with Aβ pathology in CI individuals, showed less steep increases with increasing Aβ-PET burden in the spline models, and was significantly elevated in patients with non-AD disorders. These findings suggest that plasma and CSF GFAP might be measuring partially different pathological processes, with the former being more closely related to abnormal Aβ accumulation due to AD, whereas the latter also incorporating other neuroinflammatory changes unrelated to Aβ pathology. Moreover, together with sTREM2 and YKL-40, CSF GFAP showed a lower sensitivity and specificity in detecting Aβ-positivity compared to plasma GFAP. In fact, the ability of plasma GFAP to identify Aβ-PET or CSF Aβ42/40 pathology was quite consistent across the whole sample, CU individuals, CI individuals and non-AD disorders with an area under the curve above 0.75 in all cases. These results were somewhat worse than the values obtained in two previous studies using plasma GFAP to identify a positive amyloid PET scan. In one of these studies, the analyses were conducted in cognitively normal individuals resulting in an AUC of 0.79.[15] In another study, the analyses were performed in a sample of patients with subjective cognitive complaints, mild cognitive impairment and AD dementia resulting in an AUC of 0.81.[17] The differences between our results and the ones of previous studies could potentially be related to differences in cohort characteristics. For example, in the study by Verberk et al. (2020),[17] the higher AUC value was obtained when the analyses were conducted across the entire cohort, which had many patients with AD dementia (n = 132), in contrast to our sample, which included very few AD dementia cases due to the study design (almost all patients with AD did not undergo amyloid PET imaging in BioFINDER-2). Altogether, our results suggest that plasma GFAP can be reliably used to detect Aβ-positivity across different disease stages as well as non-AD disorders. The differences between plasma and CSF GFAP could be related to different clearance pathways of the molecule into the biofluids. For instance, astrocytic end-feet projections to the neurovascular unit may provide a direct clearance pathway of the molecule into the bloodstream, and there may also be relationships with vascular amyloid pathology, which is common in AD[57].

Regarding the prognostic value of GFAP, we found that both CSF and plasma predicted global cognitive decline to the same degree, even after adjusting for changes in Aβ-PET accumulation. It has been previously suggested that, although glial responses are initially triggered by Aβ burden, they can become progressively independent of Aβ with disease

progression and contribute to neurodegenerative and cognitive changes.[55] Our findings seem to confirm this assumption as the associations between plasma GFAP and cognitive decline were still significant after adjusting for Aβ-PET burden, indicating that astrocytosis has a negative impact on cognition that goes beyond its link to Aβ pathology, in line with the findings of a recent longitudinal study.[54] This suggests that astrocytosis may play a role in promoting cognitive deterioration in AD and that therapies targeting this neuroinflammatory process could at least partially ameliorate cognitive symptoms. In addition, regarding longitudinal Aβ accumulation, we found that plasma GFAP was a better predictor of Aβ-PET burden over time, even after controlling for tau-PET signals, suggesting that plasma GFAP is a more sensitive tool to identify not only baseline but also future Aβ pathology. Finally, our mediation analyses revealed that plasma GFAP also mediated the associations between Aβ-PET and tau-PET in CU and CI individuals in a stage-dependent manner, indicating that astrocytosis might be contributing to tau accumulation, although this effect is not independent of Aβ pathology. These findings should be interpreted with caution since the mediation analysis does not allow inferring a direct causal relationship between variables, it only assesses whether amyloid PET influences plasma GFAP, which in turn influences tau PET. Thus, this analysis shows that plasma GFAP can be used to at least partially clarify the nature of the relationship between amyloid and tau. However, these findings should be confirmed by future studies in independent cohorts. If they are confirmed, they could have important implications for current treatments in AD and suggest that a combination of anti-amyloid therapies with anti-inflammatory treatments could potentially reduce the formation of tau aggregates.

Our study has several strengths, including the large number of participants with several glial biomarkers and longitudinal Aβ-PET, longitudinal tau-PET and global cognition. However, a few limitations should also be recognized such as the fact that we did not have serial longitudinal measures of plasma and CSF GFAP, which would have been useful to determine their trajectories over the course of AD and determine their potential clinical value as longitudinal monitoring tools. At the time of the study, there was only one follow-up available for Aβ-PET and two follow-ups available for cognition within a period of approximately two years. This may have limited our ability to detect stronger effects since a longer time period may be required to observe more prominent Aβ-PET and cognitive changes. Finally, the inclusion of a PET imaging tracer such as ^{11}C-deuterium-l-deprenyl[58]

would have been interesting to include to assess the relationship between plasma GFAP and regional brain astrocytosis.

In summary, here we show that baseline plasma GFAP seems to be a very early marker of astrocytosis associated with Aβ pathology suggesting it can be used to detect baseline Aβ-positivity and predict future Aβ accumulation and cognitive decline. In addition, contrary to previous assumptions, astrocytosis measured with GFAP was not associated with tau pathology after controlling for Aβ, indicating it is not only an early but also a quite specific marker for Aβ pathology. Although current models of AD have adopted a neurocentric view that starts with Aβ accumulation, followed by tau deposition and neurodegeneration, it is well known that neurons cannot function properly without the proper support of glial cells such as astrocytes.[31] Thus, our findings highlight the importance of including astroglial markers in the cascade of pathological changes occurring in AD, particularly plasma GFAP, which could potentially be used as a non-invasive tool to evaluate the effects of anti-Aβ drugs or anti-inflammatory treatments on astrocytosis in clinical trials.

Funding

The Swedish BioFINDER-2 study was supported by the Swedish Research Council (2016-00906 and 2018-02052), the Knut and Alice Wallenberg foundation (2017-0383), the Marianne and Marcus Wallenberg foundation (2015.0125), the Strategic Research Area MultiPark (Multidisciplinary Research in Parkinson's disease) at Lund University, the Swedish Alzheimer Foundation (AF-939932), the Swedish Brain Foundation (FO2019-0326), The Parkinson foundation of Sweden (1280/20), the Skåne University Hospital Foundation (2020-O000028), Regionalt Forskningsstöd (2020-0314) and the Swedish federal government under the ALF agreement (2018-Projekt0279). The precursor of 18F-flutemetamol was sponsored by GE Healthcare. The precursor of 18F-RO948 was provided by Roche. J.B.P. is supported by grants from the Swedish Research Council (#2018-02201), The Center for Medical Innovation (#20200695), a Senior Researcher Position grant at Karolinska Institute, Gamla Tjänarinnor, and Stohnes. K.B. is supported by the Swedish Research Council (#2017-00915), the Alzheimer Drug Discovery Foundation (ADDF), USA (#RDAPB-201809-2016615), the Swedish Alzheimer Foundation (#AF-742881), Hjärnfonden, Sweden (#FO2017-0243), the Swedish state under the agreement between the Swedish government and the County Councils, the ALF-agreement (#ALFGBG-715986), and European Union Joint Program for Neurodegenerative Disorders (JPND2019-466-236).

H.Z. is a Wallenberg Scholar supported by grants from the Swedish Research Council (#2018-02532), the European Research Council (#681712), Swedish State Support for Clinical Research (#ALFGBG-720931) and the UK Dementia Research Institute at UCL.

Competing interests

S.P. has served at scientific advisory boards for Geras Solutions and Hoffmann-La Roche. H.Z. has served at scientific advisory boards for Denali, Roche Diagnostics, Wave, Samumed and CogRx, has given lectures in symposia sponsored by Fujirebio, Alzecure and Biogen, and is a co-founder of Brain Biomarker Solutions in Gothenburg AB, a GU Ventures-based platform company at the University of Gothenburg. K.B. has served as a consultant or at advisory boards for Abcam, Axon, Biogen, Lilly, MagQu, Novartis and Roche Diagnostics, and is a co-founder of Brain Biomarker Solutions in Gothenburg AB, a GU Venture-based platform company at the University of Gothenburg. O.H. has acquired research support (for the institution) from AVID Radiopharmaceuticals, Biogen, Eli Lilly, Eisai, GE Healthcare, Pfizer, and Roche. In the past 2 years, he has received consultancy/speaker fees from AC Immune, Alzpath, Biogen, Cerveau and Roche. The rest of authors do not report any disclosures.

Supplementary material

Supplementary material is available at *Brain* online.

References

1. Heneka MT, Carson MJ, El Khoury J *et al.* Neuroinflammation in Alzheimer's disease. *Lancet Neurol.* 2015;14:388-405.

2. Osborn LM, Kamphuis W, Wadman WJ, Hol EM. Astrogliosis: an integral player in the pathogenesis of Alzheimer's disease. Prog Neurobiol. 2016;144:121-41.

3. Itagaki S, McGeer PL, Akiyama H, Zhu S, Selkoe D. Relationship of microglia and astrocytes to amyloid deposits of Alzheimer disease. *J Neuroimmunology.* 1989;24:173-82.

4. Frost GR, Li YM. The role of astrocytes in amyloid production and Alzheimer's disease. Open Biol. 2017;7:170228.

5. Beach TG, McGeer EG. Lamina-specific arrangement of astrocytic gliosis and senile plaques in Alzheimer's disease visual cortex. *Brain Res.* 1988;463:357-61.

6. Perez-Nievas BG, Serrano-Pozo A. Deciphering the astrocyte reaction in Alzheimer's disease. *Front Aging Neurosci.* 2018;10:114.

7. Ikeda K, Haga C, Akiyama H, Kase K, Iritani S. Coexistence of paired helical filaments and glial filaments in astrocytic processes within ghost tangles. *Neurosci Lett.* 1992;148:126-8.

8. Ikeda K, Haga C, Oyanagi S, Iritani S, Kosaka K. Ultrastructural and immunohistochemical study of degenerate neurite-bearing ghost tangles. *J Neurol.* 1992;239:191-4.

9. Simpson JE, Ince PG, Lace G *et al.* Astrocyte phenotype in relation to Alzheimer-type pathology in the ageing brain. *Neurobiol Aging.* 2010;31:578-90.

10. Rajan KB, Aggarwal NT, McAninch EA *et al.* Remote Blood Biomarkers of Longitudinal Cognitive Outcomes in a Population Study. *Ann Neurol.* 2020;88:1065-76.

11. Oeckl P, Halbgebauer S, Anderl-Straub S *et al.* Glial fibrillary acidic protein in serum is increased in Alzheimer's disease and correlates with cognitive impairment. *J Alzh Dis.* 2019;67:481-8.

12. Elahi FM, Casaletto KB, La Joie R et al. Plasma biomarkers of astrocytic and neuronal dysfunction in early-and late-onset Alzheimer's disease. *Alzheimers & Dem.* 2019;16:681-95.

13. Thijssen EH, Verberk IM, Stoops E, Boxer AL, Teunissen CE. Amyloid, pTau, NfL, and GFAP as biomarkers for Alzheimer's disease: Clinical study results of AD blood biomarkers. *Alzheimers & Dem.* 2020;16:e038179.

14. Asken BM, Elahi FM, La Joie R *et al.* Plasma Glial Fibrillary Acidic Protein Levels Differ Along the Spectra of Amyloid Burden and Clinical Disease Stage. *J Alzh Dis.* 2020; In press.

15. Chatterjee P, Pedrini S, Stoops E et al. Plasma glial fibrillary acidic protein is elevated in cognitively normal older adults at risk of Alzheimer's disease. Trans Psych. 2021;11:27.

16. Cicognola C, Janelidze S, Hertze J *et al.* Plasma Glial Fibrillary Acidic Protein Detects Alzheimer Pathology and Predicts Future Conversion to Alzheimer Dementia in Patients With Mild Cognitive Impairment. *Alzheimers Res Ther* 2021; In press.

17. Verberk IM, Thijssen E, Koelewijn J et al. Combination of plasma amyloid beta (1-42/1-40) and glial fibrillary acidic protein strongly associates with cerebral amyloid pathology. *Alzheimers Res Ther* 2020;12:1-4.

18. Simrén J, Leuzy A, Karikari TK et al. The diagnostic and prognostic capabilities of plasma biomarkers in Alzheimer's disease. *Alzheimers & Dem* 2021; In press.

19. Busche MA, Hyman BT. Synergy between amyloid-β and tau in Alzheimer's disease. Nat Neurosci. 2020;23:1183-93.

20. Gratuze M, Leyns CE, Holtzman DM. New insights into the role of TREM2 in Alzheimer's disease. *Mol Neurodegen.* 2018;13:1-6.

21. Ulland T K, Colonna M. TREM2—a key player in microglial biology and Alzheimer disease. *Nat Rev Neurol.* 2018;14,667-75.

22. Henjum K, Almdahl IS, Årskog V, *et al.* Cerebrospinal fluid soluble TREM2 in aging and Alzheimer's disease. *Alzheimers Res Ther.* 2016;8:1-11.

23. Kleinberger G, Yamanishi Y, Suárez-Calvet M, *et al.* TREM2 mutations implicated in neurodegeneration impair cell surface transport and phagocytosis. *Sci Transl Med.* 2014;6:243ra86.

24. Piccio L, Deming Y, Del-Águila JL, *et al.* Cerebrospinal fluid soluble TREM2 is higher in Alzheimer disease and associated with mutation status. *Acta Neuropathol.* 2016;131:925-33.

25. Heslegrave A, Heywood W, Paterson R, *et al.* Increased cerebrospinal fluid soluble TREM2 concentration in Alzheimer's disease. *Mol Neurodegener.* 2016;11: 1-7.

26. Suárez-Calvet M, Kleinberger G, Araque Caballero MÁ, *et al.* sTREM2 cerebrospinal fluid levels are a potential biomarker for microglia activity in early-stage Alzheimer's disease and associate with neuronal injury markers. *EMBO Mol Med.* 2016;8:466-76.

27. Carmona S, Zahs K, Wu E, Dakin K, Bras J, Guerreiro R. The role of TREM2 in Alzheimer's disease and other neurodegenerative disorders. *Lancet Neurol.* 2018;17:721-30.

28. Rauchmann BS, Schneider-Axmann T, Alexopoulos P, Perneczky R, Alzheimer's Disease Neuroimaging Initiative. CSF soluble TREM2 as a measure of immune response along the Alzheimer's disease continuum. *Neurobiol Aging.* 2019;74:182-90.

29. Ewers M, Franzmeier N, Suárez-Calvet M, *et al.* Increased soluble TREM2 in cerebrospinal fluid is associated with reduced cognitive and clinical decline in Alzheimer's disease. *Sci Trans Med.* 2019;11(507).

30. Rathcke CN, Vestergaard H. YKL-40, a new inflammatory marker with relation to insulin resistance and with a role in endothelial dysfunction and atherosclerosis. *Inflamm Res.* 2006;55:221–7.

31. Shao R, Hamel K, Petersen L *et al.* YKL-40, a secreted glycoprotein, promotes tumor angiogenesis. *Oncogene.* 2009;28:4456-68.

32. Johansen JS. Studies on serum YKL-40 as a biomarker in diseases with inflammation, tissue remodelling, fibroses and cancer. *Dan Med Bull.* 2006;53:172-209.

33. Villar-Piqué A, Schmitz M, Hermann P *et al.* Plasma YKL-40 in the spectrum of neurodegenerative dementia. *J Neuroinflamm.* 2019;16:1-5.

35. Baldacci F, Lista S, Cavedo E, Bonuccelli U, Hampel H. Diagnostic function of the neuroinflammatory biomarker YKL-40 in Alzheimer's disease and other neurodegenerative diseases. *Expert Rev Proteomics.* 2017;14:285-99.

36. Lleó A, Alcolea D, Martínez-Lage P *et al.* Longitudinal cerebrospinal fluid biomarker trajectories along the Alzheimer's disease continuum in the BIOMARKAPD study. *Alzheimers Dement.* 2019;15:742-53.

37. Palmqvist S, Insel PS, Stomrud E *et al.* Cerebrospinal fluid and plasma biomarker trajectories with increasing amyloid deposition in Alzheimer's disease. *EMBO Mol Med.* 2019;11:e11170.

38. Janelidze S, Mattsson N, Stomrud E *et al.* CSF biomarkers of neuroinflammation and cerebrovascular dysfunction in early Alzheimer disease. *Neurology.* 2018;91(9):e867-77.

39. Schindler SE, Li Y, Todd KW *et al.* Emerging cerebrospinal fluid biomarkers in autosomal dominant Alzheimer's disease. *Alzheimers Dement.* 2019;15:655-65.

40. Palmqvist S, Janelidze S, Quiroz YT *et al.* Discriminative accuracy of plasma phospho-tau217 for Alzheimer disease vs other neurodegenerative disorders. *JAMA.* 2020;324:772-81.

41. Palmqvist S, Janelidze S, Stomrud E *et al.* Performance of fully automated plasma assays as screening tests for alzheimer disease–related b-amyloid status. *JAMA Neurol.* 2019;76:1060-9.

42. Bertens D, Tijms BM, Scheltens P, Teunissen CE, Visser PJ. Unbiased estimates of cerebrospinal fluid beta-amyloid 1-42 cutoffs in a large memory clinic population. *Alzheimers Res Ther.* 2017;9:8.

43. Landau SM, Fero A, Baker SL et al. Measurement of longitudinal β-amyloid change with 18F-florbetapir PET and standardized uptake value ratios. J Nucl Med. 2015;56:567-74.

44. Ossenkoppele R, Rabinovici GD, Smith R *et al.* Discriminative accuracy of [18F] flortaucipir positron emission tomography for Alzheimer disease vs other neurodegenerative disorders. *JAMA.* 2018;320:1151-62.

45. Cho H, Choi JY, Hwang MS *et al.* In vivo cortical spreading pattern of tau and amyloid in the Alzheimer disease spectrum. *Ann Neurol.* 2016;80:247-58.

46. Palmqvist S, Insel PS, Stomrud E *et al.* Cerebrospinal fluid and plasma biomarker trajectories with increasing amyloid deposition in Alzheimer's disease. *EMBO Mol Med.* 2019;11:e11170.

47. Jack Jr CR, Knopman DS, Jagust WJ *et al.* Tracking pathophysiological processes in Alzheimer's disease: an updated hypothetical model of dynamic biomarkers. *Lancet Neurol.* 2013;12:207-16.

48. Benjamini Y, Hochberg Y. Controlling the false discovery rate: a practical and powerful approach to multiple testing. *J Royal Stat Soc Series B*. 1995;57:289-300.

49. Chumbley J, Worsley K, Flandin G, Friston K. Topological FDR for neuroimaging. *Neuroimage*. 2010;49:3057-964.

50. Medeiros R, LaFerla FM. Astrocytes: conductors of the Alzheimer disease neuroinflammatory symphony. *Exp Neurol.* 2013;239:133-8.

51. Carter SF, Herholz K, Rosa-Neto P, Pellerin L, Nordberg A, Zimmer ER. Astrocyte biomarkers in Alzheimer’s disease. *Trends Mol Med.* 2019;25:77-95.

52. Olsson B, Lautner R, Andreasson U *et al.* CSF and blood biomarkers for the diagnosis of Alzheimer's disease: a systematic review and meta-analysis. *Lancet Neurol.* 2016;15:673-84.

53. Van Hulle C, Jonaitis EM, Betthauser TJ *et al.* An examination of a novel multipanel of CSF biomarkers in the Alzheimer's disease clinical and pathological continuum. *Alzheimers Dement.* 2020; In press.

54. Verberk IM, Laarhuis MB, van den Bosch KA et al. Serum markers glial fibrillary acidic protein and neurofilament light for prognosis and monitoring in cognitively normal older people: a prospective memory clinic-based cohort study. *Lancet Healthy Long.* 2021;2:e87-95.

55. Serrano-Pozo A, Mielke ML, Gómez-Isla T *et al.* Reactive glia not only associates with plaques but also parallels tangles in Alzheimer's disease. *Am J Pathol.* 2011;179:1373-84.

56. Lemoine L, Saint-Aubert L, Nennesmo I, Gillberg PG, Nordberg A. Cortical laminar tau deposits and activated astrocytes in Alzheimer's disease visualised by 3 H-THK5117 and 3 H-deprenyl autoradiography. *Sci Rep.* 2017;7:1-1.

57. Bourassa P, Tremblay C, Schneider JA, Bennett DA, Calon F. Beta-amyloid pathology in human brain microvessel extracts from the parietal cortex: relation with cerebral amyloid angiopathy and Alzheimer's disease. *Acta Neuropathol.* 2019;137:801-23.

58. Rodriguez-Vieitez E, Carter SF, Chiotis K *et al.* Comparison of early-phase 11C-deuterium-l-deprenyl and 11C-Pittsburgh compound B PET for assessing brain perfusion in Alzheimer disease. *J Nucl Med.* 2016;57:1071-7.

Figure Legends

Figure 1. Plasma and CSF GFAP concentrations are increased in Aβ-positive groups

Violin plots with median values for plasma and CSF GFAP (z scores) in Aβ-negative cognitively unimpaired individuals (CU Aβ-), Aβ-positive cognitively unimpaired individuals (CU Aβ+), Aβ-positive cognitively impaired individuals (CI Aβ+), Aβ-negative cognitively impaired individuals (CI Aβ-) and non-AD disorders, after adjusting for age and sex. * Indicates significant group differences after adjusting for multiple comparisons with FDR corrections ($q < 0.05$).

Figure 2. Plasma and CSF GFAP concentrations are associated with Aβ-PET independently of tau-PET burden

Results of the linear regression analyses showing a significant relationship between Aβ burden measured on positron emission tomography (Aβ-PET) (z scores) and plasma GFAP (z scores) in A) all cognitively unimpaired individuals (CU), B) Aβ-negative cognitively unimpaired individuals (CU Aβ-), C) Aβ-positive cognitively unimpaired individuals (CU Aβ+), and D) Aβ-positive cognitively impaired individuals (CI Aβ+), after adjusting for age and sex. In addition, a significant relationship between Aβ-PET and CSF GFAP (z scores) was also found in E) Aβ-positive cognitively unimpaired individuals (CU Aβ+). The upper panel shows correlation plots between Aβ-PET and GFAP markers, whereas the lower panel shows boxplots depicting how Aβ-PET values vary according to GFAP quartiles. All associations remained significant after controlling for tau-PET burden.

Figure 3. Voxel-wise associations between plasma GFAP and Aβ-PET

Results of the voxel-wise regression analyses showing a significant relationship between Aβ burden measured on positron emission tomography images and plasma GFAP in A) all cognitively unimpaired individuals (CU) and B) Aβ-positive cognitively unimpaired individuals (CU Aβ+), and D) Aβ-positive cognitively impaired individuals (CI Aβ+), after adjusting for age and sex. All results were adjusted for multiple comparisons using FDR ($q < 0.05$).

Figure 4. Plasma GFAP shows early increases with Aβ-PET burden

Spline models showing the trajectories for A) plasma GFAP and B) CSF GFAP using global Aβ-PET SUVR as a proxy for time. Both models were significant; however, when the splines of plasma and CSF GFAP were compared, plasma GFAP showed steeper initial increases, overcoming CSF GFAP levels even before Aβ-PET positivity (C).

Figure 5. Plasma GFAP has a greater diagnostic accuracy in identifying an Aβ-positive status compared to other glial markers

Results of the receiver operating curve analyses showing that plasma GFAP showed a better classification performance in distinguishing Aβ-PET positive from Aβ-PET negative individuals in the A) whole sample, B) all cognitively unimpaired individuals (CU) and C) all Aβ-positive cognitively impaired individuals (CI). Moreover, plasma GFAP also showed a better classification performance in distinguishing patients with abnormal and normal CSF Aβ42/40 levels in a group of patients with non-AD disorders (D). AUC, area under the curve.

Figure 6. Relationship between plasma and CSF GFAP with longitudinal Aβ accumulation and cognitive decline

Predicted trajectories for longitudinal Aβ accumulation determined by PET and mini-mental state scores (MMSE) (z scores) in relation to plasma and CSF GFAP in the whole sample, after adjusting for covariates. The models were fit using continuous GFAP values but for illustration purposes the plots show the trajectories for individuals with high and low plasma GFAP for longitudinal Aβ-PET (A) and longitudinal MMSE (B) as well as for individuals with high and low CSF GFAP for longitudinal MMSE (C). All results were adjusted for multiple comparisons using FDR ($q < 0.05$).

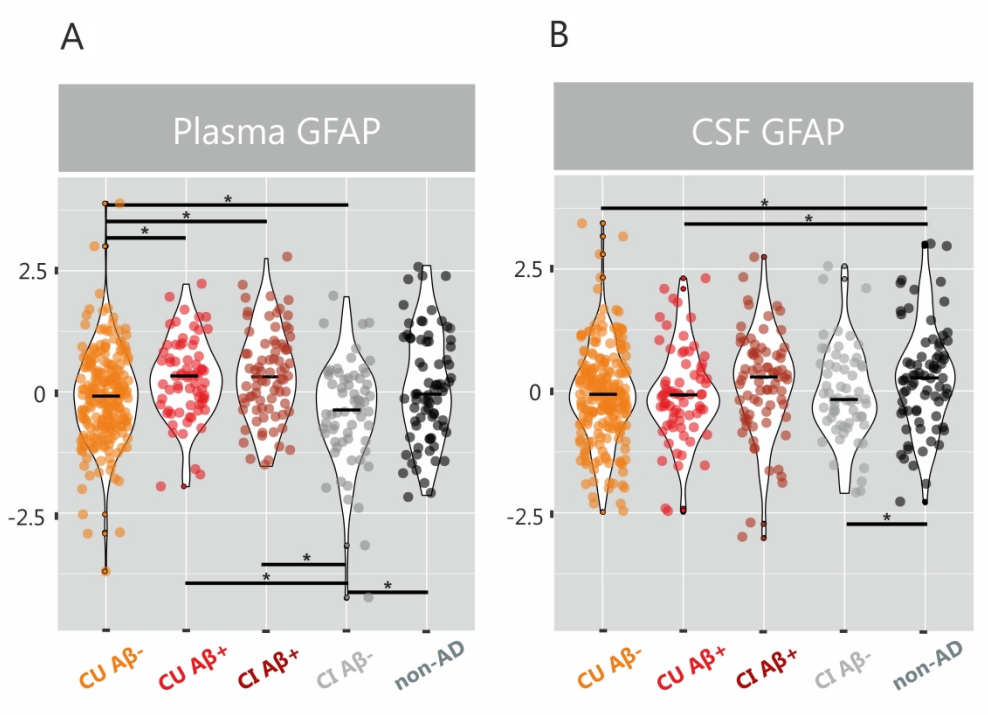

Figure 1. Plasma and CSF GFAP concentrations are increased in Aβ-positive groups.
Violin plots with median values for plasma and CSF GFAP (z scores) in Aβ-negative cognitively unimpaired individuals (CU Aβ-), Aβ-positive cognitively unimpaired individuals (CU Aβ+), Aβ-positive cognitively impaired individuals (CI Aβ+), Aβ-negative cognitively impaired individuals (CI Aβ-) and non-AD disorders, after adjusting for age and sex. * Indicates significant group differences after adjusting for multiple comparisons with FDR corrections ($q < 0.05$).

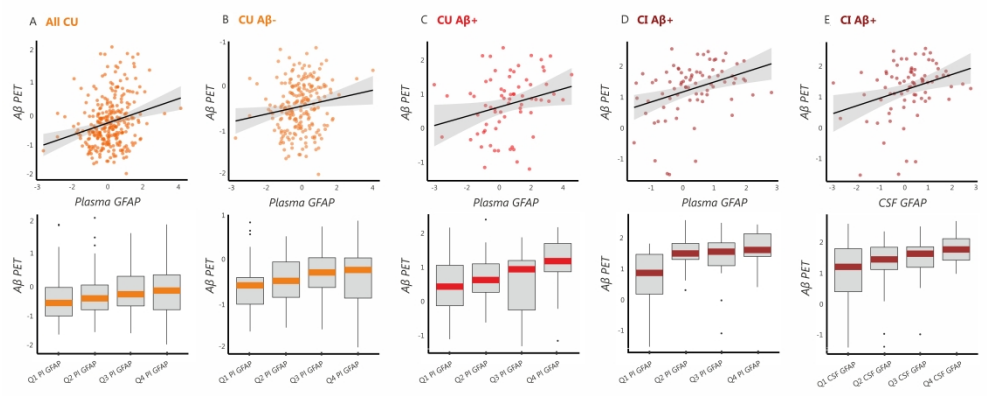

Figure 2. Plasma and CSF GFAP concentrations are associated with Aβ-PET independently of tau-PET burden. Results of the linear regression analyses showing a significant relationship between Aβ burden measured on positron emission tomography (Aβ-PET) (z scores) and plasma GFAP (z scores) in A) all cognitively unimpaired individuals (CU), B) Aβ-negative cognitively unimpaired individuals (CU Aβ-), C) Aβ-positive cognitively unimpaired individuals (CU Aβ+), and D) Aβ-positive cognitively impaired individuals (CI Aβ+), after adjusting for age and sex. In addition, a significant relationship between Aβ-PET and CSF GFAP (z scores) was also found in E) Aβ-positive cognitively unimpaired individuals (CU Aβ+). The upper panel shows correlation plots between Aβ-PET and GFAP markers, whereas the lower panel shows boxplots depicting how Aβ-PET values vary according to GFAP quartiles. All associations remained significant after controlling for tau-PET burden.

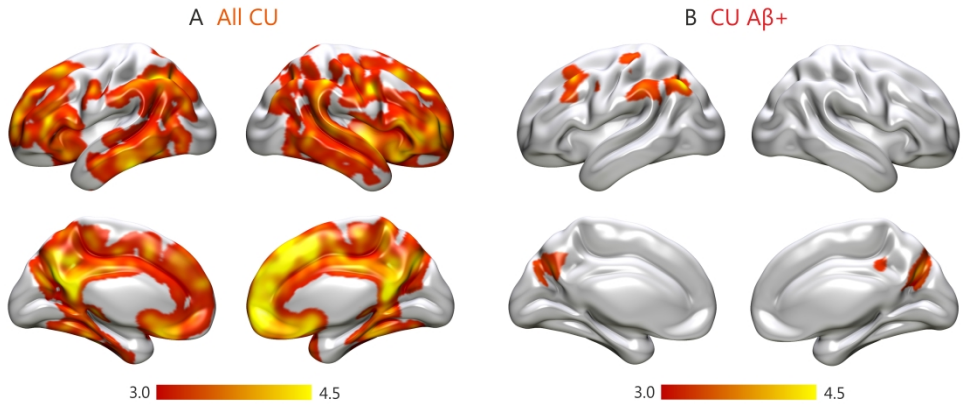

Figure 3. Voxel-wise associations between plasma GFAP and Aβ-PET.
Results of the voxel-wise regression analyses showing a significant relationship between Aβ burden measured on positron emission tomography images and plasma GFAP in A) all cognitively unimpaired individuals (CU) and B) Aβ-positive cognitively unimpaired individuals (CU Aβ+), and D) Aβ-positive cognitively impaired individuals (CI Aβ+), after adjusting for age and sex. All results were adjusted for multiple comparisons using FDR ($q < 0.05$).

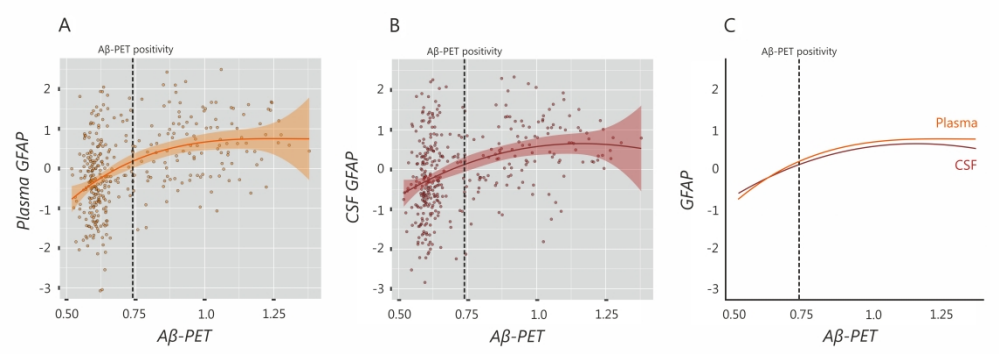

Figure 4. Plasma GFAP shows early increases with Aβ-PET burden.
Spline models showing the trajectories for A) plasma GFAP and B) CSF GFAP using global Aβ-PET SUVR as a proxy for time. Both models were significant; however, when the splines of plasma and CSF GFAP were compared, plasma GFAP showed steeper initial increases, overcoming CSF GFAP levels even before Aβ-PET positivity (C).

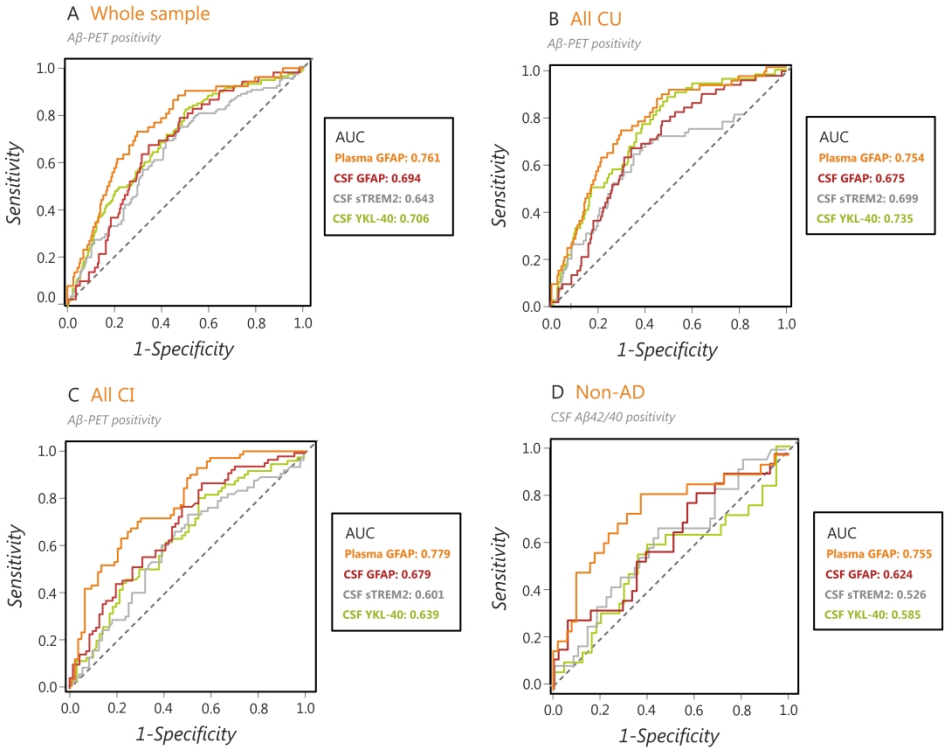

Figure 5. Plasma GFAP has a greater diagnostic accuracy in identifying an Aβ-positive status compared to other glial markers.
Results of the receiver operating curve analyses showing that plasma GFAP showed a better classification performance in distinguishing Aβ-PET positive from Aβ-PET negative individuals in the A) whole sample, B) all cognitively unimpaired individuals (CU) and C) all Aβ-positive cognitively impaired individuals (CI). Moreover, plasma GFAP also showed a better classification performance in distinguishing patients with abnormal and normal CSF Aβ42/40 levels in a group of patients with non-AD disorders (D). AUC, area under the curve.

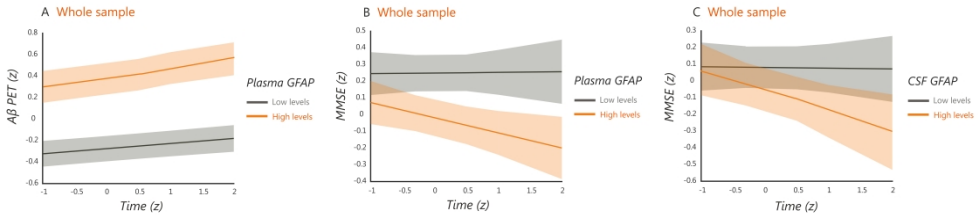

Figure 6. Relationship between plasma and CSF GFAP with longitudinal Aβ accumulation and cognitive decline.

Predicted trajectories for longitudinal Aβ accumulation determined by PET and mini-mental state scores (MMSE) (z scores) in relation to plasma and CSF GFAP in the whole sample, after adjusting for covariates. The models were fit using continuous GFAP values but for illustration purposes the plots show the trajectories for individuals with high and low plasma GFAP for longitudinal Aβ-PET (A) and longitudinal MMSE (B) as well as for individuals with high and low CSF GFAP for longitudinal MMSE (C). All results were adjusted for multiple comparisons using FDR ($q < 0.05$).

Table 1 Baseline sample characteristics

	CU Aβ- (*n* = 217)	CU Aβ+ (*n* = 71)	CI Aβ+ (*n* = 78)	CI Aβ– (*n* = 63)	Non-AD (*n* = 75)	*P*-value
Age	63.8 (41.2–87.9)	72.1 (51.0–88.7)	73.0 (53.7–93.3)	67.9 (45.2–83.4)	73.5 (52.5–87.3)	<0.001
Sex, male/female	98/119	35/36	34/44	36/27	50/25	0.369
Education	12.4 (6–25)	11.5 (7–19)	13.0 (6–33)	11.9 (7–20)	11.6 (7–22)	0.069
MMSE	28.9 (26–30)	28.9 (24–30)	26.5 (18–30)	27.3 (23–30)	23.1 (10–30)	<0.001
APOE ε4 (%)	38.7	70.4	76.9	28.6	31	<0.001
CSF Aβ42/40	1.1 (0.8–1.4)	0.55 (0.3–0.7)	0.52 (0.3–0.7)	1.1 (0.8–1.5)	0.92 (0.4–1.3)	<0.001
Plasma GFAP (pg/ml)	179.6 (31.1–534.9)	252.1 (86.1–672.9)	262.6 (94.0–650.7)	166.9 (24.5–476.0)	241.7 (76.6–823.7)	<0.001
CSF GFAP (pg/ml)	13.5 (4.3–34.6)	16.1 (5.8–35.1)	17.7 (5.5–35.6)	14.7 (5.4–31.2)	18.4 (8.2–40.6)	<0.001
CSF YKL40 (ng/ml)[a]	162.0 (38.3–458.2)	211.2 (80.9–374.8)	220.3 (63.9–523.5)	184.6 (68.1–371.0)	221.1 (79.3–517.8)	<0.001
CSF sTREM2 (ng/ml)[b]	10.3 (4.9–22.9)	12.3 (4.7–21.9)	11.5 (5.5–29.6)	10.8 (6.2–24.7)	12.2 (6.7–20.1)	<0.001
Global Aβ-PET SUVR	0.61 (0.5–0.9)	0.85 (0.6–1.3)	1.0 (0.6–1.4)	0.62 (0.5–0.7)	–	<0.001
Braak I-II Tau-PET SUVR	1.1 (0.8–1.4)	1.28 (0.9–1.9)	1.6 (1.0–3.1)	1.13 (0.9–1.5)	1.3 (0.8–3.3)	<0.001
Braak III-IV Tau-PET SUVR	1.1 (0.9–1.3)	1.20 (1.0–1.6)	1.5 (1.0–3.2)	1.14 (0.8–1.3)	1.2 (0.9–2.0)	<0.001
Braak V-VI Tau-PET SUVR	1.0 (0.8–1.3)	1.0 (0.8–1.2)	1.2 (0.9–1.8)	1.02 (0.7–1.2)	1.0 (0.7–1.5)	<0.001

Data presented in the table correspond to medians followed by (range). P-values were derived from Kruskal Wallis tests for continuous non-normally distributed measures and Chi-squared tests for categorical measures. MMSE, Mini-Mental State Examination; CSF, cerebrospinal fluid; GFAP, glial fibrillary acidic protein; YKL-40, chitinase 3-like 1; sTREM2, soluble triggering receptor expressed on myeloid cells 2; SUVR, standard uptake value ratio; PET, positron emission tomography; pg/mL, picograms per milliliter; ng/ml, nanograms per milliliter.

[a]YKL-40 values were missing for 2 subjects (1 CU Aβ+, 1 CI Aβ+).

[b]sTREM2 values were missing for 2 subjects (1 CI Aβ+, 1 non-AD patient).

Table 2 Diagnostic accuracy of plasma and CSF biomarkers to detect Aβ- positivity on PET or CSF Aβ42/40

	AUC	Accuracy	Sensitivity	Specificity
Whole sample				
Plasma GFAP	0.761	70.6%	71.3%	70.4%
CSF GFAP **	0.694	60.1%	81.2%	51.8%
CSF sTREM2 ***	0.643	61.5%	68.6%	58.6%
CSF YKL-40	0.706	59.5%	83.5%	50.0%
All CU individuals				
Plasma GFAP	0.754	70.8%	73.1%	70.3%
CSF GFAP *	0.675	66.0%	67.3%	65.7%
CSF sTREM2	0.699	61.8%	78.9%	58.1%
CSF YKL-40	0.735	57.5%	88.5%	50.6%
All CI individuals				
Plasma GFAP	0.779	70.9%	71.4%	70.4%
CSF GFAP *	0.679	65.3%	87.1%	43.7%
CSF sTREM2 **	0.601	61.4%	73.9%	49.3%
CSF YKL-40 **	0.639	62.9%	81.2%	45.1%
Non-AD patients				
Plasma GFAP	0.755	70.0%	83.3%	62.8%
CSF GFAP	0.624	73.3%	29.2%	94.1%
CSF sTREM2	0.526	60.0%	58.3%	60.8%
CSF YKL-40 *	0.585	58.1%	66.7%	54.0%

The analyses conducted in the whole sample, CU and CI individuals were performed using Aβ-PET, whereas the analyses conducted in a separate non-AD group were performed using CSF Aβ42/40. CU, cognitively unimpaired; CI, cognitively impaired; AD, Alzheimer's disease; AUC, area under the curve; GFAP, glial fibrillary acidic protein; CSF, cerebrospinal fluid; sTREM2, soluble triggering receptor expressed on myeloid cells 2; YKL-40, chitinase 3-like 1.

*p < 0.05 vs plasma GFAP.

**p < 0.01 vs plasma GFAP.

***p < 0.001 vs plasma GFAP.